

Dual Cross-Linked Hydrogels: Linear Rheology and Fractional Calculus Modeling

Agniva Dutta^a, Valeriy V. Ginzburg^{b,*}, Gleb Vasilyev^a, and Eyal Zussman^{a,*}

^a NanoEngineering Group, Faculty of Mechanical Engineering, Technion-Israel Institute of Technology, Haifa 3200003, Israel

^b Department of Chemical Engineering and Materials Science, Michigan State University, East Lansing, Michigan 48224, USA

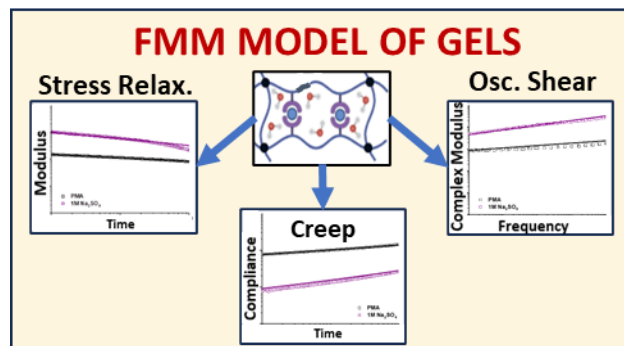
* Corresponding author emails: ginzbur7@msu.edu (VVG), meeyal@me.technion.ac.il (EZ)

ABSTRACT

Hydrogels are increasingly recognized as a versatile platform for applications spanning from tissue engineering to soft robotics or flexible electronics. Recent efforts have focused on enhancing and tailoring their mechanical performance to meet application-specific demands. However, the intricate viscoelastic response of hydrogels remains challenging to capture using conventional phenomenological models. In this study, we prepared a series of tough dual crosslinked hydrogels - poly(methacrylamide-co-acrylic acid)-Fe³⁺ and systematically tuned their mechanical properties by leveraging the salting-out effect. The viscoelastic behavior of the hydrogels was characterized under shear deformations, and a four-parameter Fractional Maxwell Model (FMM) was constructed to quantitatively describe oscillatory shear, creep, and stress relaxation responses. The influence of salt concentration on each FMM parameter was analyzed and correlated with bulk mechanical performance. This framework provides a first step toward capturing the complex viscoelastic nature of the advanced hydrogels and lays the foundation for developing more comprehensive nonlinear constitutive models.

Keywords: Hydrogel, Fractional Maxwell Model, Viscoelasticity, Dual crosslinked hydrogel, Salting out

For Table of Contents use only



1. INTRODUCTION

Hydrogels, composed of crosslinked polymer networks swollen with water, closely resemble biological tissues and hold great promise for emerging technologies such as soft robotics,^{1,2} wearable/flexible electronics,^{3,4} sensors,^{5,6} and energy storage devices.^{7,8} A wide range of these applications demands hydrogels that can withstand substantial static and dynamic loads while resisting premature failure. Therefore, tailoring their mechanical properties to meet specific performance requirements is critical for practical implementation. Conventional hydrogels are inherently weak and brittle, primarily due to severe stress localization under load, often resulting in premature fracture. To overcome these limitations, various toughening strategies have been developed, primarily based on stress delocalization.⁹ A widely adopted approach involves incorporating energy-dissipative motifs into the hydrogel network. These motifs preferentially break before the primary polymer backbone, dissipating applied energy and delaying catastrophic failure. Restoration of such motifs after breaking is essential to recover mechanical integrity, which is typically achieved using reversible physical bonds/interactions as crosslinkers.¹⁰ Strategies beyond dissipation-based mechanisms can enhance material toughness by enabling the elastic absorption of energy. For example, slide-ring hydrogels incorporate figure-of-eight polyrotaxane crosslinks that can move freely along polymer chains, redistributing stress like pulleys.¹¹ This sliding mechanism effectively increases the chain length between crosslinks, improving extensibility. It is also possible for dense entanglements in swollen polyacrylamide hydrogels to slip due to reduced friction in water.¹² Unlike conventional covalent crosslinks, these mobile entanglements prevent premature fracture by distributing stress at crack tips.

Most reported hydrogels are viscoelastic, incorporating an additional design dimension, time, through their temporal structure. This temporal component is governed by the lifetime of cross-links, and even subtle changes in cross-linking kinetics can markedly influence bulk mechanical properties.¹³ Notably, the mechanical response of soft materials often exhibits complexities that extend beyond the scope of classical phenomenological models, including the Maxwell, Kelvin-Voigt, or Zener (standard linear solid) frameworks. These traditional models, which combine Hookean springs and Newtonian dashpots, capture linear viscoelasticity but fail to account for the power-law scaling frequently observed in hydrogel material functions such as relaxation modulus and creep compliance. The Burgers model, which couples Maxwell with a Kelvin-Voigt element in a series, extends this frame to describe creep and stress relaxation. However, it remains constrained by discrete relaxation times and thus fails to capture broad relaxation spectra of hydrogels.^{14,15} This deviation arises from the broad distribution of structural length scales and relaxation times inherent to the hydrogels. Consequently, a comprehensive understanding of both spatial and temporal design elements is essential for rationally tuning the hydrogel's mechanical properties.

In recent years, many problems dealing with systems having broad relaxation time distributions have been successfully addressed using the fractional calculus methods.^{16–32} In particular, fractional viscoelastic models, which employ fractional derivatives instead of conventional first-order terms, provide a concise framework for describing complex mechanical responses. These models inherently capture power-law relaxation and broad time spectra, offering advantages over classical approaches such as generalized Maxwell model (“Prony series”) which require multiple elements. Several of these studies were devoted to hydrogels. Jaishankar and McKinley used their Fractional Maxwell Gel (FMG) model to successfully describe the power-

law stress relaxation in food hydrogels (caseinate and alginate).^{22,25} Ruso and coworkers compared classical and fractional rheological models for hydroxyapatite-based composite hydrogels and found that the fractional models more accurately described their time-dependent viscoelastic behavior.³³ Miranda-Valdez and coworkers similarly applied fractional viscoelastic models to conventional cellulose-based hydrogels, successfully capturing frequency-dependent viscoelastic responses across varying concentrations.³⁴ Lenocho et al. further combined fractional and generalized Maxwell models to describe the thermorheological behavior of poly(acrylic acid)-Fe(III) hydrogels, observing a transition in relaxation mechanism dominated by chain dynamics to the dissociation of coordination crosslinks as gelation progressed.³⁵ Despite these advances, fractional viscoelastic models remain largely unexplored in the context of advanced, mechanically tunable hydrogels. This gap underscores the need for modeling approaches tailored to hydrogel systems with mechanical properties tunable across a broad spectrum.

In this study, we employed the Fractional Maxwell Model (FMM) to analyze the viscoelastic behavior of a dual cross-linked poly(methacrylamide-co-acrylic acid)-Fe³⁺ (PMA) hydrogel.³⁶ The dual-crosslinking strategy integrates permanent covalent crosslinks with dynamic Fe³⁺-acrylic acid coordination bond crosslinks, the latter breaking preferentially under external loading to dissipate energy.³⁷ To tune the mechanical properties across a broad spectrum, we exploited the salting-out effect by immersing the hydrogels in sodium sulfate solutions of varying concentrations. The mechanical response of both pristine and salt-treated PMA hydrogels was systematically examined under shear deformation, and a four-parameter FMM model was constructed to capture the oscillatory shear, creep, and stress relaxation behaviors.

2. MATERIALS AND METHODS

2.1 Materials. Methacrylamide (MAAm) and ammonium persulfate (APS) were purchased from Sigma Aldrich. Acrylic acid (AAc) was purchased from Merck, and N,N,N',N'-tetramethylethylenediamine (TEMED) from Acros Organics. Ferric nitrate nonahydrate $[\text{Fe}(\text{NO}_3)_3 \cdot 9\text{H}_2\text{O}]$ was purchased from Fisher Scientific, and anhydrous Sodium sulfate (Na_2SO_4) from Bio-lab Ltd. All chemicals were used as received without further purification.

2.2 Preparation of the Poly(MAAm-co-AAc)- Fe^{3+} hydrogel. The dual crosslinked hydrogel was prepared through a conventional three-step procedure.^{36,37}

Step 1 - Synthesis of chemically crosslinked hydrogel:

MAAm (2.4 M), AAc (10 mol% relative to MAAm), and MBAA (0.06 mol% relative to the total monomer content) were dissolved in deionized water. The solution was purged with nitrogen gas for 15 min to remove dissolved oxygen. Subsequently, initiator APS (1 wt.% relative to total monomer weight) and accelerator TEMED (20 μL) were added under constant stirring. The resulting solution was slowly poured into a Teflon mold and allowed to polymerize at room temperature for 12 h to obtain chemically crosslinked hydrogels.

Step 2 - Ionic crosslinking with Fe^{3+} :

The chemically crosslinked hydrogels were immersed in a 0.06 M $\text{Fe}(\text{NO}_3)_3$ solution for 24 h to introduce ionic crosslinking via Fe^{3+} coordination with carboxylic groups.

Step 3 - Post-treatment:

The hydrogel samples were immersed in a large volume of deionized water for 48 h, with the water being replaced periodically to remove excess Fe^{3+} . Finally, the hydrogels were treated with sodium sulfate solution of varying molarities to get the final dual crosslinked hydrogels.

2.3 Characterization. The mechanical properties of the hydrogels under shear deformation were characterized using a Discovery DHR-2 rheometer (TA Instruments, USA) equipped with a parallel plate geometry (20 mm diameter, 1.4-1.7 mm gap). To prevent slippage during testing, 240-grit waterproof sandpaper was affixed to the plate surfaces. Frequency sweep experiments were carried out at room temperature ($T = 25\text{ }^{\circ}\text{C}$) within the linear viscoelastic region, determined by preliminary amplitude sweep test. (See Figure S1 in the Supporting Information for more details). The strain amplitude was 0.04%, and the frequency range was between 0.1 and 100 rad/s for the oscillatory shear. Stress-relaxation measurements were performed at $25\text{ }^{\circ}\text{C}$, by applying an instantaneous strain and recording the stress decay over a 12 min period. The values of applied strain belonged to the linear viscoelastic region and varied in the range 0.06 - 0.6% depending on the Na_2SO_4 molarity. Creep tests were carried out by continuous shearing of samples at a constant stress for 5 min at $25\text{ }^{\circ}\text{C}$. The values of applied stress varied in the range 200 - 400 Pa depending on the Na_2SO_4 molarity.

2.4 Modeling – the Fractional Maxwell Model (FMM) for Linear Viscoelasticity. To model the linear viscoelasticity of the gels, we utilize the Fractional Maxwell Model (FMM), schematically shown in **Figure 1**.

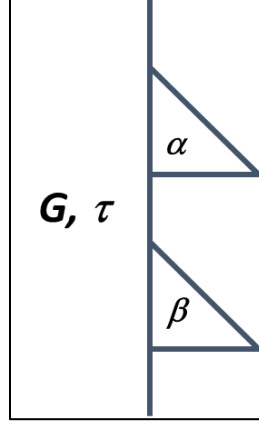


Figure 1. Schematic representation of the Fractional Maxwell Model (FMM). The two triangles represent two Scott Blair elements connected in series. See text for more details.

As proposed by McKinley and co-workers,^{21,23,25,26,28} the linear viscoelasticity of gels and other complex fluids can be described based on the power-law Scott Blair^{38–40} (SB) elements. Each individual SB element (represented as a triangle in Figure 1) can be thought of as a representation of a material with an infinitely broad relaxation spectrum. In particular, the linear viscoelastic storage and loss moduli of an SB element are given by,

$$G'(\omega) = G \cos \left[\frac{\pi\beta}{2} \right] (\omega\tau)^\beta \quad (1a)$$

$$G''(\omega) = G \sin \left[\frac{\pi\beta}{2} \right] (\omega\tau)^\beta \quad (1b)$$

Here, G , τ , and β are the modulus, relaxation time, and power-law exponent of the SB element, respectively. Note that for $\beta = 0.5$, $G' = G''$ for all frequencies ω . Thus, SB element with $\beta = 0.5$ describes the “ideal Winter-Chambon” gel.^{41–44} The SB elements with $0 < \beta < 0.5$ describe the “solid-like” gels, with $\beta = 0$ corresponding to the classical Hookean spring. The SB elements with $0.5 < \beta < 1$ describe the “liquid-like” gels, with $\beta = 1$ corresponding to the classical Maxwell dashpot. In the FMM, two SB elements are connected in series and have the same G and τ , but

different power-law exponents α and β . It is generally assumed that $0 \leq \beta < \alpha \leq 1$. The storage and loss moduli of the FMM are given by,

$$\frac{G'(\omega)}{G} = \frac{(\omega\tau)^\alpha \cos\left(\frac{\pi\alpha}{2}\right) + (\omega\tau)^{2\alpha-\beta} \cos\left(\frac{\pi\beta}{2}\right)}{1 + (\omega\tau)^{\alpha-\beta} \cos\left(\frac{\pi(\alpha-\beta)}{2}\right) + (\omega\tau)^{2(\alpha-\beta)}} \quad (2a)$$

$$\frac{G''(\omega)}{G} = \frac{(\omega\tau)^\alpha \sin\left(\frac{\pi\alpha}{2}\right) + (\omega\tau)^{2\alpha-\beta} \sin\left(\frac{\pi\beta}{2}\right)}{1 + (\omega\tau)^{\alpha-\beta} \cos\left(\frac{\pi(\alpha-\beta)}{2}\right) + (\omega\tau)^{2(\alpha-\beta)}} \quad (2b)$$

The creep compliance, $J(t)$, can likewise be easily described in elementary functions,²¹

$$J(t) = \frac{1}{G} \left[\frac{1}{\Gamma(1+\alpha)} \left(\frac{t}{\tau}\right)^\alpha + \frac{1}{\Gamma(1+\beta)} \left(\frac{t}{\tau}\right)^\beta \right] \quad (3)$$

where $\Gamma(x)$ is the gamma-function.

The stress relaxation, $G(t)$, can be obtained as an inverse Fourier transform of the complex modulus $G^*(\omega) = G'(\omega) + iG''(\omega)$. Although it cannot be expressed in elementary functions, $G(t)$ can be described using the so-called Mittag-Leffler special function, $E_{a,b}(x)$,²⁵

$$G(t) = G \left(\frac{t}{\tau}\right)^{-\beta} E_{1-\alpha, 1-\beta} \left[-\left(\frac{t}{\tau}\right)^{\alpha-\beta} \right] \quad (4a)$$

where,

$$E_{a,b}[x] = \sum_{k=0}^{\infty} \frac{x^k}{\Gamma(ak+b)} \quad (4b)$$

Thus, if a complex system (such as a polymer gel) can be described by a single FMM, the three independent experiments (stress relaxation, creep, and frequency sweep) can be captured using only four parameters: G , τ , α , and β . The parameterization procedure is described next.

2.5. Modeling -- The Model Parameter Optimization Procedure. We attempt to minimize the following objective function characterizing the difference between the experimental data and the model fit:

$$\Omega = w_{SR}\Omega_{SR} + w_C\Omega_C + w_{FS}\Omega_{FS} \quad (5a)$$

Here, the indices SR, C, and FS stand for “stress relaxation”, “creep”, and “frequency sweep”, respectively; w_i are the weights associated with each of the three experiments. We choose $w_{CR} = w_C = w_{FS} = 0.333$. The individual objective functions Ω_{SR} , Ω_C , and Ω_{FS} are given by,

$$\Omega_{SR} = \frac{1}{N_{SR}} \sum_{k=1}^{N_{SR}} \left| \log \frac{G[k]_{exp}}{G_{model}(t[k])} \right| \quad (5b)$$

$$\Omega_C = \frac{1}{N_C} \sum_{k=1}^{N_C} \left| \log \frac{J[k]_{exp}}{J_{model}(t[k])} \right| \quad (5c)$$

$$\Omega_{FS} = \frac{1}{N_{FS}} \sum_{k=1}^{N_{FS}} \left| \log \frac{|G^*_{exp}|[k]}{|G^*_{model}|(\omega[k])} \right| \quad (5d)$$

Here, $k = 1, N_i$, $i = SR, C$, or FS , corresponds to the index of a specific data point in the experimental array, and N_i are the array lengths (numbers of points); $Y_{exp}[k]$ are the experimental data, with $Y = G$ (for SR), J (for C), and $|G^*|$ (for FS). The \log operator means a base-10 logarithm. The complex modulus magnitude is given by,

$$|G^*| = \sqrt{(G')^2 + (G'')^2} \quad (6)$$

The model values $G_{model}(t)$ are given by equations 4a – 4b, $J_{model}(t)$ by equation 3, and $|G^*_{model}|(\omega)$ by equations 2a, 2b, and 6.

The ranges used for optimization are 1 – 100 s for the creep and stress relaxation experiments, and 0.1 – 100 s⁻¹ for the oscillatory shear experiments. The parameter optimization is then done in Microsoft Excel 2019 using the Generalized Reduced Gradient (GRG) procedure.

3. RESULTS AND DISCUSSION

3.1 The Two Networks. In Figure 2, we schematically show the structure of the prepared hydrogels. There are two types of effective crosslinks in the hydrogels - the covalent bonds (black dots) and the ionic physical crosslinks (blue circles with purple semicircles). The overall viscoelastic response of the hydrogel depends on the relative density of the two types of crosslinks. As discussed in our previous papers,^{36,45} the addition of salt causes the phase separation of excess water, making the hydrogels stiffer. Increasing the salt concentration leads to increased phase separation (“syneresis”), and a substantial increase in the gel modulus and strength.

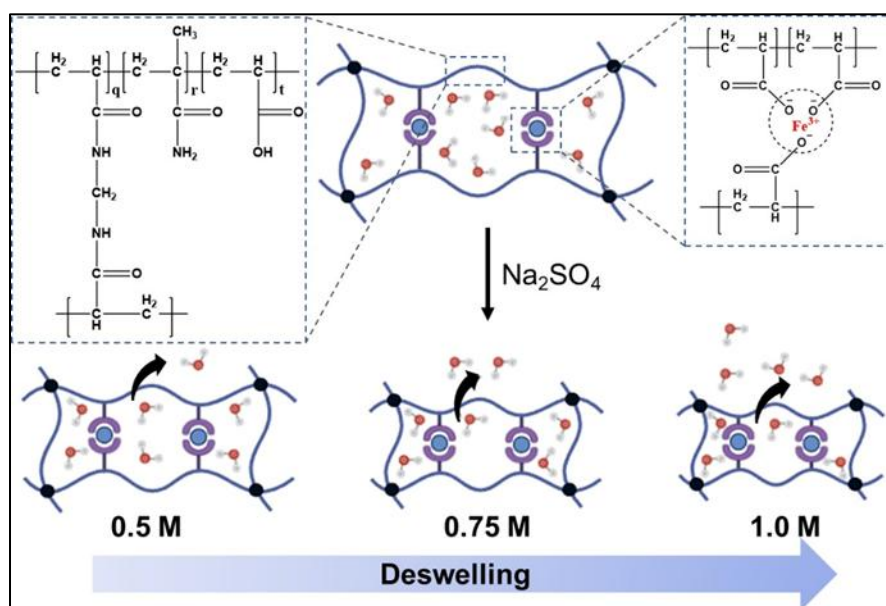


Figure 2. The chemistry of the hydrogels, two types of crosslinks, and the syneresis occurring due to the addition of the sodium sulphate salt.

Because of the two different crosslink types, it is appropriate to use the Fractional Maxwell Model (FMM) as the “minimum model” to describe the linear viscoelasticity of the gels. We

performed the FMM parameterization of the viscoelastic measurements for the five PMA gels with varying salt content. The results are discussed below.

3.2 Stress Relaxation. The stress relaxation (SR) experiment describes the time-dependent shear modulus, $G(t)$, as a function of time after one applies an instantaneous strain and records the stress decay; the time-dependent shear modulus is the ratio of the time-dependent stress to the (constant) strain. The experimental data and corresponding FMM model fits are shown in Figure 3a for the no-salt PMA and 1M Na_2SO_4 PMA gels, and in Figure 3b for all the intermediate salt concentrations. (The FMM model parameters are summarized in Table 1 at the end of this section).

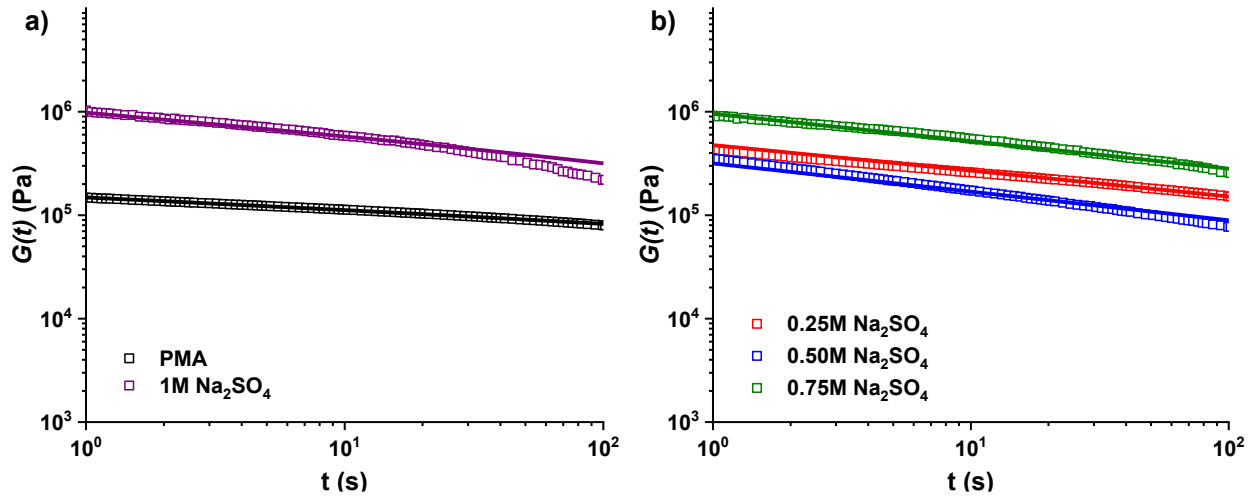


Figure 3. Stress relaxation experiments data (symbols) and FMM model fits (solid lines). (a) Pure PMA with no salt (black), and PMA with 1M Na_2SO_4 (purple) (b) PMA with 0.25M (red), 0.5M (blue), and 0.75M (green) of Na_2SO_4 .

One can draw several conclusions from the figures. First, the FMM fits provide very good descriptions of the relaxation data, at least within the time range considered in our analysis (1 – 100 s). The high-salt 1M Na_2SO_4 system is one exception – at large times, it shows a deviation from the model prediction, relaxing faster than expected. This can perhaps be explained by some weakly nonlinear effects and/or by spontaneous break-up of various clusters – the processes not

captured within the FMM framework. Second, the stress-relaxation curves show a fairly complex behavior, especially for the intermediate (0.25M, 0.5M, and 0.75M) salt concentrations. The initial modulus seems to exhibit a plateau for the salt concentrations in the 0.25M – 0.5M, while the slope of the modulus decay (on a log-log scale) seems to exhibit a non-monotonic behavior for the intermediate salt concentrations. We will examine the possible explanations for these phenomena later in this section.

3.3 Creep. The creep test measures the time-dependent deformation of the gel sample subjected to a constant load; the deformation is then converted to creep compliance, J . The experimental and FMM fitting results for the creep test are shown in Figures 4a and 4b (similar groupings as in Figure 3). In this case as well, the FMM model fits well with the data. The FMM parameters are the same as for the stress relaxation experiments (Table 1).

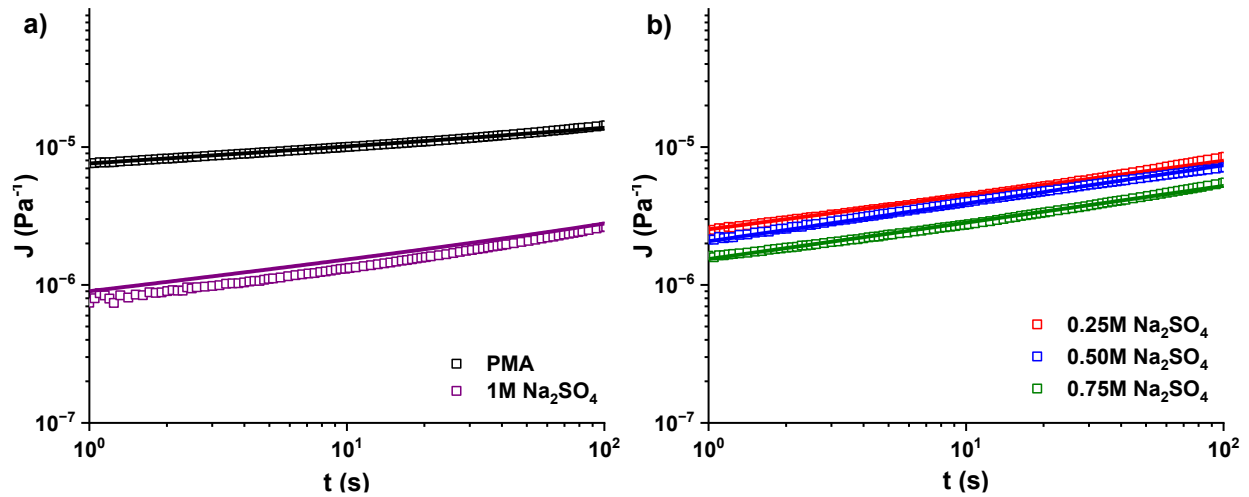


Figure 4. Creep experiments data (symbols) and FMM model fits (solid lines). (a) Pure PMA with no salt (black), and PMA with 1M Na_2SO_4 (purple) (b) PMA with 0.25M (red), 0.5M (blue), and 0.75M (green) of Na_2SO_4 .

Creep compliance is in some ways the inverse of the modulus, so the higher-compliance materials are the softer ones, and the lower-compliance ones are the stiffer gels. Again, as

expected, the intermediate-salt-concentration (0.25M and 0.5M) gels exhibit very similar behaviors, as do the higher-salt-concentration ones (0.75M and 1M).

3.4 Oscillatory Shear Modulus. To fit our model, we did not use the storage and loss moduli separately, but rather the overall complex modulus amplitude, $|G^*|$ (equation 6). The results are plotted in Figures 5a and 5b.

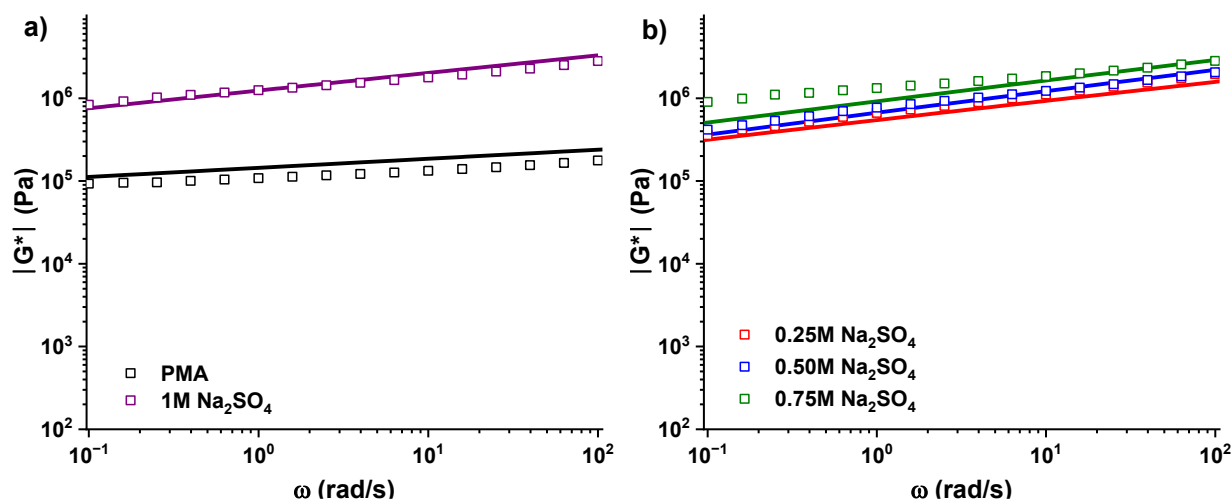


Figure 5. Frequency sweep experiments data (symbols) and FMM model fits (solid lines). (a) Pure PMA with no salt (black), and PMA with 1M Na_2SO_4 (purple) (b) PMA with 0.25M (red), 0.5M (blue), and 0.75M (green) of Na_2SO_4 .

The comparison between the model and the FMM fits shows reasonable agreement, except for the 0.75M salt gel at low frequencies. The dependence of the complex modulus amplitude on the frequency is approximately – but not exactly – a power-law (which is a signature of a Scott Blair element). The dependence of $|G^*|$ on the salt concentration is monotonic, with the gel rigidity increasing upon the addition of the salt, as one would expect.^{36,45} The model parameters are the same as for the other two cases (Table 1).

3.5 Salt Concentration Dependence of the Model Parameters. The FMM model parameters are summarized in Table 1 for all five gels considered here, and their dependence on the salt content is depicted in Figures 6a – 6d. The estimated standard errors are: 0.2 for $\log(G, \text{Pa})$ and $\log(\tau, \text{s})$, and 0.03 for α and β .

Table 1. FMM model parameters for different salt concentrations: logarithm of the shear modulus, G ; large power-law exponent, α ; small power-law exponent, β ; logarithm of the relaxation time, τ ; the objective function, Ω . See text for more details.

Sample	PMA	0.25M Na₂SO₄	0.5M Na₂SO₄	0.75M Na₂SO₄	1.0M Na₂SO₄
Log G (Pa)	4.58	4.75	4.56	5.05	5.33
Log τ (s)	5.3	4.7	5.24	4.1	3.6
α (-)	0.38	0.31	0.33	0.32	0.68
β (-)	0.11	0.22	0.24	0.24	0.21
Ω (-)	0.045	0.037	0.052	0.037	0.080

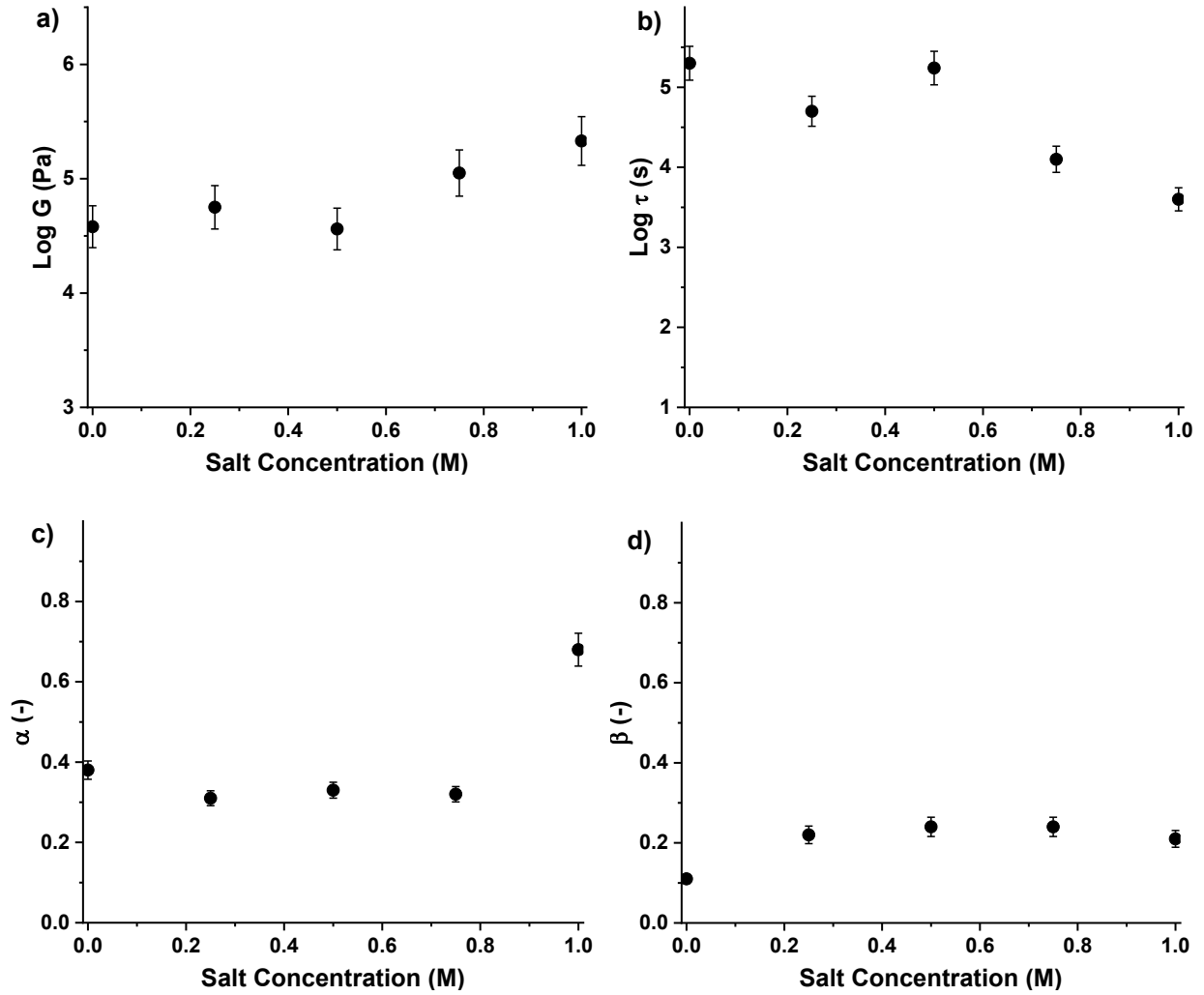


Figure 6. Salt concentration dependence of the FMM model parameters. (a) Logarithm of the shear modulus, G ; (b) logarithm of the relaxation time, τ ; (c) large power-law exponent, α ; (d) small power-law exponent, β . See text for more details.

Physical interpretation of the FMM parameters is still a challenge, given that an FMM is a simplified representation of a complex fluid with multiple relaxation modes corresponding to various structures. Still, we can offer a tentative analysis of the trends seen in Figures 6a – 6d. The overall trend revealed that the modulus magnitude, G (Figure 6a) increased with rising salt concentration, consistent with previous observations where stiffness and strength were enhanced as a function of salt concentration.³⁶ The increase in modulus, which reflects the effective

crosslinking density, can be attributed to salt-induced deswelling that forces polymer chains towards high energy conformations. Since the mechanical properties of hydrogels are often governed by the lifetime of physical cross-links, systems with slow binding/unbinding kinetics are expected to exhibit higher strength, whereas fast exchange rates yield softer gels. Interestingly, in PMA hydrogels, while the modulus increased with salt concentration, the overall relaxation time (τ) decreased (Figure 6b). Previously, cyclic tensile loading–unloading tests demonstrated that the hysteresis area, representing the energy dissipation relative to toughness, increased markedly with salt concentration.³⁶ Together, we can tentatively stipulate that the ionic crosslinks are forced into more “rigid”, higher-energy conformations in the higher-salt-concentration gels. Accordingly, at low deformations, the barrier to escape those conformations becomes smaller, and the stress is transferred to weaker physical crosslinks, making them more prone to rupture, reducing their lifetime. The trends in the exponents α (Figure 6c) and β (Figure 6d) are even more difficult to explain fully. A Maxwell model – whether classical or fractional – describes two elements in series, so their displacements are summed up. The first element – characterized by the exponent α – is supposed to be “more compliant”, especially at long times ($t \gg \tau$). At low-to-intermediate salt concentrations, $0.3 < \alpha < 0.4$, corresponding to a viscoelastic material similar to a “post-gel”.^{41,42,46,47} At high salt concentration, however, the exponent α increases sharply ($\alpha \approx 0.7$), and the first element is now more similar to a “pre-gel”.^{42,46–48} The second element – characterized by the exponent β – is the “more elastic” one. A “perfectly elastic” element would have $\beta = 0$; here, we estimate $0.1 < \beta < 0.3$, indicating a strong “post-gel”. Comparing the two extremes, pristine PMA versus PMA at 1 M salt concentration, both α and β nearly doubled. The rise in α suggests an increasingly liquid-like response in the first element, while the increase in β reflects a reduction in elasticity of the second element. Toughness could be defined as the sum of dissipated and

elastically stored energy. As observed in cyclic tensile tests, higher salt concentrations increased the relative contribution of energy dissipation compared to elastic storage. This aligns well with variations noted in the values of the two power exponents. Interestingly, for the intermediate salt concentrations, α and β are relatively close. This might suggest that those gels could even be analyzed using a single Scott Blair element, and their creep would be almost an ideal power-law function of time. For both high and low salt content, there appears to be a separation into two distinct rheological elements. The physical meaning of this separation is still uncertain and requires further analysis.

3.6 Discussion. The fractional Maxwell model (FMM) analysis of several PMA-based ionic gels prepared with different salt concentrations shows an interesting and complex rheological behavior. The characterization included three separate measurements – stress relaxation (SR), creep (C), and oscillatory shear (OS). Within some relatively well-defined time (for C and SR) or frequency (OS) ranges, FMM provides a reasonably good four-parameter description of all three tests. There have been very few examples where a single fractional model can capture these tests simultaneously (see, e.g., Aime et al.⁴⁹). Thus, the current analysis offers further support for the idea that fractional calculus models can provide a parsimonious and physically meaningful description of the linear rheology of complex fluids (including hydrogels).

The physical meaning of the two Scott Blair elements is, at present, somewhat obscure (and this is a challenge for many rheological models, including classical Maxwell or generalized Maxwell models). The two elements might correspond to two separate but interpenetrating – or microphase-separated – networks. We observe that the properties of the two elements are more or less similar depending on the salt concentration – is this a signature of some viscoelastic

(micro)phase separation? Are there other tools (complementary to rheology) that could further elucidate these phenomena? These are questions for future studies.

There are a number of other questions that are not fully answered by the current model. For example, the stress relaxation accelerates at long times, and this behavior is not captured within a single FMM. Adding new elements would probably improve the agreement between model and experiment, but at the cost of introducing new parameters with no clear physical meaning. Is the enhanced relaxation at longer times due to the spontaneous bond-breaking not tied to the built-in strain? Or are there nonlinear effects in play? Likewise, are the discrepancies between the model and experiment in the low-frequency region for the OS experiment due to the failure of the model, potential nonlinearity, or some other factors? We will be exploring these topics in the future.

Finally, it is important to note that the linear tests – as important as they are – are only the first step in the evaluation of the hydrogels and prediction of their properties and application performance. The FMM models parameterized here should be considered a stepping stone *en route* to building a comprehensive nonlinear dynamic stress-strain model.^{22,24,25,45}

4. CONCLUSIONS

We characterized the linear rheology of PMA-based ionic hydrogels and modeled it using the fractional Maxwell model (FMM) approach. A simple four-parameter FMM model is shown to successfully capture the oscillatory shear, creep, and stress relaxation experiments. We investigated the dependence of the model parameters on the salt concentration and found interesting and non-trivial dependencies that will be investigated in the future. The calculated FMM model parameters will be used to develop the dynamic nonlinear stress-strain models.

ASSOCIATED CONTENT

Supporting Information

The Supporting Information is available free of charge at:

Description of the amplitude sweep to determine the boundaries of the linear regime for the linear oscillatory shear measurements.

AUTHOR INFORMATION

Corresponding Authors:

Valeriy V. Ginzburg, Department of Chemical Engineering and Materials Science, Michigan State University, East Lansing, Michigan 48224, USA. Email ginzbur7@msu.edu

Eyal Zussman, NanoEngineering Group, Faculty of Mechanical Engineering, Technion-Israel Institute of Technology, Haifa 3200003, Israel

Authors:

Agniva Dutta, NanoEngineering Group, Faculty of Mechanical Engineering, Technion-Israel Institute of Technology, Haifa 3200003, Israel

Gleb Vasilyev, NanoEngineering Group, Faculty of Mechanical Engineering, Technion-Israel Institute of Technology, Haifa 3200003, Israel

Notes:

The authors declare no competing financial interest.

ACKNOWLEDGMENTS

V.G. thanks the Faculty of Mechanical Engineering, Technion, Israel, for hospitality and support during his sabbatical. E.Z. acknowledges the financial support of the Winograd Chair of Fluid Mechanics and Heat Transfer at Technion.

REFERENCES

- (1) Lee, Y.; Song, W. J.; Sun, J. Y. Hydrogel Soft Robotics. *Materials Today Physics* **2020**, *15*, 100258. <https://doi.org/10.1016/j.mtphys.2020.100258>.
- (2) Naranjo, A.; Martín, C.; López-Díaz, A.; Martín-Pacheco, A.; Rodríguez, A. M.; Patiño, F. J.; Herrero, M. A.; Vázquez, A. S.; Vázquez, E. Autonomous Self-Healing Hydrogel with Anti-Drying Properties and Applications in Soft Robotics. *Appl Mater Today* **2020**, *21*. <https://doi.org/10.1016/j.apmt.2020.100806>.
- (3) Hu, L.; Chee, P. L.; Sugiarto, S.; Yu, Y.; Shi, C.; Yan, R.; Yao, Z.; Shi, X.; Zhi, J.; Kai, D.; Yu, H.; Huang, W. Hydrogel-Based Flexible Electronics. *Advanced Materials* **2023**, *35* (14). <https://doi.org/10.1002/adma.202205326>.
- (4) Ji, C.; Wang, Y.; Qi, Q.; Li, Y.; Cao, L. Electrically Conductive Hydrogels for Flexible Wearable Devices: Materials, Design, and Applications. *Adv Mater Technol* **2025**. <https://doi.org/10.1002/admt.202501044>.
- (5) Dutta, A.; Panda, P.; Das, A.; Ganguly, D.; Chattopadhyay, S.; Banerji, P.; Pradhan, D.; Das, R. K. Intrinsically Freezing-Tolerant, Conductive, and Adhesive Proton Donor-Acceptor Hydrogel for Multifunctional Applications. *ACS Appl Polym Mater* **2022**, *4* (10), 7710–7722. <https://doi.org/10.1021/acsapm.2c01285>.
- (6) Das, S.; Martin, P.; Vasilyev, G.; Nandi, R.; Amdursky, N.; Zussman, E. Processable, Ion-Conducting Hydrogel for Flexible Electronic Devices with Self-Healing Capability. *Macromolecules* **2020**, *53* (24), 11130–11141. <https://doi.org/10.1021/acs.macromol.0c02060>.
- (7) Dutta, A.; Ghosal, K.; Sarkar, K.; Pradhan, D.; Das, R. K. From Ultrastiff to Soft Materials: Exploiting Dynamic Metal–Ligand Cross-Links to Access Polymer Hydrogels Combining

- Customized Mechanical Performance and Tailorable Functions by Controlling Hydrogel Mechanics. *Chemical Engineering Journal* **2021**, 419. <https://doi.org/10.1016/j.cej.2021.129528>.
- (8) Chao, D.; Zhou, W.; Xie, F.; Ye, C.; Li, H.; Jaroniec, M.; Qiao, S.-Z. Roadmap for Advanced Aqueous Batteries: From Design of Materials to Applications. *Sci Adv* **2020**, 6 (21), 2375–2548. <https://doi.org/10.1126/sciadv.aba4098>.
- (9) Li, X.; Gong, J. P. Design Principles for Strong and Tough Hydrogels. *Nat Rev Mater* **2024**, 9 (6), 380–398. <https://doi.org/10.1038/s41578-024-00672-3>.
- (10) Dutta, A.; Pandit, S.; Panda, P.; Das, R. K. Competitive (Spatiotemporal) Techniques to Fabricate (Ultra)Stiff Polymer Hydrogels and Their Potential Applications. *ACS Applied Polymer Materials*. American Chemical Society March 28, 2025, pp 3466–3497. <https://doi.org/10.1021/acsapm.4c04199>.
- (11) Okumura, Y.; Ito, K. The Polyrotaxane Gel: A Topological Gel by Figure-of-Eight Cross-Links. *Advanced Materials* **2001**, 13 (7), 485–487. [https://doi.org/10.1002/1521-4095\(200104\)13:7<485::AID-ADMA485>3.0.CO;2-T](https://doi.org/10.1002/1521-4095(200104)13:7<485::AID-ADMA485>3.0.CO;2-T).
- (12) Kim, J.; Zhang, G.; Shi, M.; Suo, Z. Fracture, Fatigue, and Friction of Polymers in Which Entanglements Greatly Outnumber Cross-Links. *Science (1979)* **2021**, 374 (6564), 212–216. <https://doi.org/10.1126/science.abg6320>.
- (13) Sun, W.; Xue, B.; Fan, Q.; Tao, R.; Wang, C.; Wang, X.; Li, Y.; Qin, M.; Wang, W.; Chen, B.; Cao, Y. Molecular Engineering of Metal Coordination Interactions for Strong, Tough, and Fast-Recovery Hydrogels. *Sci Adv* **2020**, 6 (16), 1–12. <https://doi.org/10.1126/sciadv.aaz9531>.

- (14) Suriano, R.; Griffini, G.; Chiari, M.; Levi, M.; Turri, S. Rheological and Mechanical Behavior of Polyacrylamide Hydrogels Chemically Crosslinked with Allyl Agarose for Two-Dimensional Gel Electrophoresis. *J Mech Behav Biomed Mater* **2014**, *30*, 339–346. <https://doi.org/10.1016/j.jmbbm.2013.12.006>.
- (15) Dutta, A.; Vasilyev, G.; Zussman, E. Thermoregulation of Hydrogel Spatiotemporal Mechanics by Exploiting the Folding–Unfolding Characteristics of Globular Proteins. *Biomacromolecules* **2023**, *24* (6), 2575–2586. <https://doi.org/10.1021/acs.biomac.3c00073>.
- (16) Macías-Díaz, J. E. Fractional Calculus—Theory and Applications. *Axioms* **2022**, *11* (2), 43.
- (17) Barbero, G.; Evangelista, L. R.; Zola, R. S.; Lenzi, E. K.; Scarfone, A. M. A Brief Review of Fractional Calculus as a Tool for Applications in Physics: Adsorption Phenomena and Electrical Impedance in Complex Fluids. *Fractal and Fractional* **2024**, *8* (7), 369.
- (18) Yavuz, M.; Özdemir, N. *Fractional Calculus: New Applications in Understanding Nonlinear Phenomena*; Bentham Science Publishers: Singapore, 2022; Vol. 3.
- (19) Dingyü, X.; Lu, B. *Fractional Calculus High-Precision Algorithms and Numerical Implementations*; Springer: Singapore, 2024.
- (20) Zayernouri, M.; Wang, L.-L.; Shen, J.; Karniadakis, G. E. *Spectral and Spectral Element Methods for Fractional Ordinary and Partial Differential Equations*; Cambridge University Press: Cambridge, 2024. <https://doi.org/DOI: 10.1017/9781108867160>.
- (21) Jaishankar, A.; McKinley, G. H. Power-Law Rheology in the Bulk and at the Interface: Quasi-Properties and Fractional Constitutive Equations. *Proceedings of the Royal Society A: Mathematical, Physical and Engineering Sciences* **2013**, *469* (2149), 20120284.

- (22) Jaishankar, A.; McKinley, G. H. A Fractional K-BKZ Constitutive Formulation for Describing the Nonlinear Rheology of Multiscale Complex Fluids. *J Rheol (N Y N Y)* **2014**, *58* (6), 1751–1788.
- (23) Faber, T. J.; Jaishankar, A.; McKinley, G. H. Describing the Firmness, Springiness and Rubberiness of Food Gels Using Fractional Calculus. Part I: Theoretical Framework. *Food Hydrocoll* **2017**, *62*, 325–339.
- (24) Keshavarz, B.; Divoux, T.; Manneville, S.; McKinley, G. H. Nonlinear Viscoelasticity and Generalized Failure Criterion for Polymer Gels. *ACS Macro Lett* **2017**, *6* (7), 663–667.
- (25) Rathinaraj, J. D. J.; McKinley, G. H.; Keshavarz, B. Incorporating Rheological Nonlinearity into Fractional Calculus Descriptions of Fractal Matter and Multi-Scale Complex Fluids. *Fractal and Fractional* **2021**, *5* (4), 174.
- (26) Song, J.; Holten-Andersen, N.; McKinley, G. H. Non-Maxwellian Viscoelastic Stress Relaxations in Soft Matter. *Soft Matter* **2023**, *19* (41), 7885–7906.
- (27) Das, M.; Rathinaraj, J. D. J.; Palade, L. I.; McKinley FRS, G. H. Laun’s Rule for Predicting the First Normal Stress Coefficient in Complex Fluids: A Comprehensive Investigation Using Fractional Calculus. *Physics of Fluids* **2024**, *36* (1), 13111. <https://doi.org/10.1063/5.0179709>.
- (28) Wagner, C. E.; Barbati, A. C.; Engmann, J.; Burbidge, A. S.; McKinley, G. H. Quantifying the Consistency and Rheology of Liquid Foods Using Fractional Calculus. *Food Hydrocoll* **2017**, *69*, 242–254.
- (29) D’Elia, M.; Zayernouri, M.; Gulian, M.; Suzuki, J. *Fractional Modeling in Action: A Survey of Nonlocal Models for Subsurface Transport, Turbulent Flows, and Anomalous Materials*; 2021. <https://doi.org/10.13140/RG.2.2.13264.43526>.

- (30) Tzelepis, D. A.; Khoshnevis, A.; Zayernouri, M.; Ginzburg, V. V. Polyurea–Graphene Nanocomposites—The Influence of Hard-Segment Content and Nanoparticle Loading on Mechanical Properties. *Polymers (Basel)* **2023**, *15* (22), 4434.
- (31) Suzuki, J. L.; Zayernouri, M.; Bittencourt, M. L.; Karniadakis, G. E. Fractional-Order Uniaxial Visco-Elasto-Plastic Models for Structural Analysis. *Comput Methods Appl Mech Eng* **2016**, *308*, 443–467.
- (32) Tzelepis, D. A.; Suzuki, J.; Su, Y. F.; Wang, Y.; Lim, Y. C.; Zayernouri, M.; Ginzburg, V. V. Experimental and Modeling Studies of IPDI-Based Polyurea Elastomers – The Role of Hard Segment Fraction. *J Appl Polym Sci* **2023**, *140* (10), e53592. <https://doi.org/https://doi.org/10.1002/app.53592>.
- (33) Cambeses-Franco, P.; Rial, R.; Ruso, J. M. Integrating Classical and Fractional Calculus Rheological Models in Developing Hydroxyapatite-Enhanced Hydrogels. *Physics of Fluids* **2024**, *36* (7). <https://doi.org/10.1063/5.0213561>.
- (34) Puente-Córdova, J. G.; Rentería-Baltíerrez, F. Y.; Miranda-Valdez, I. Y. Fractional Rheology as a Tool for Modeling Viscoelasticity in Cellulose-Based Hydrogels. *Cellulose* **2025**, *32* (6), 3619–3632. <https://doi.org/10.1007/s10570-025-06468-0>.
- (35) Lenocho, A.; Schönhoff, M.; Cramer, C. Modelling Viscoelastic Relaxation Mechanisms in Thermorheologically Complex Fe(III)-Poly(Acrylic Acid) Hydrogels. *Soft Matter* **2022**, *18* (44), 8467–8475. <https://doi.org/10.1039/d2sm01122k>.
- (36) Dutta, A.; Maity, P.; Das, R. K.; Zussman, E. Molecular Engineering of Backbone Rotation in an Energy-Dissipative Hydrogel for Combining Ultra-High Stiffness and Toughness. *Mater Horiz* **2025**, *12* (13), 4901–4914. <https://doi.org/10.1039/D4MH01717J>.

- (37) Lin, P.; Ma, S.; Wang, X.; Zhou, F. Molecularly Engineered Dual-Crosslinked Hydrogel with Ultrahigh Mechanical Strength, Toughness, and Good Self-Recovery. *Advanced Materials* **2015**, *27* (12), 2054–2059. <https://doi.org/10.1002/adma.201405022>.
- (38) Rogosin, S.; Mainardi, F. George William Scott Blair--the Pioneer of Fractional Calculus in Rheology. *arXiv preprint arXiv:1404.3295* **2014**.
- (39) Blair, G. W. S. The Role of Psychophysics in Rheology. *J Colloid Sci* **1947**, *2* (1), 21–32.
- (40) Blair, G. W. S.; Veinoglou, B. C.; Caffyn, J. E. Limitations of the Newtonian Time Scale in Relation to Non-Equilibrium Rheological States and a Theory of Quasi-Properties. *Proc R Soc Lond A Math Phys Sci* **1947**, *189* (1016), 69–87.
- (41) Winter, H. H.; Chambon, F. Analysis of Linear Viscoelasticity of a Crosslinking Polymer at the Gel Point. *J Rheol (N Y N Y)* **1986**, *30* (2), 367–382.
- (42) Chambon, F.; Winter, H. H. Linear Viscoelasticity at the Gel Point of a Crosslinking PDMS with Imbalanced Stoichiometry. *J Rheol (N Y N Y)* **1987**, *31* (8), 683–697.
- (43) Larson, R. G. *The Structure and Rheology of Complex Fluids*; Oxford university press New York, 1999; Vol. 150.
- (44) Rubinstein, M.; Colby, R. H. *Polymer Physics*; 2003.
- (45) Goswami, M.; Dutta, A.; Kulshreshtha, R.; Vasilyev, G.; Zussman, E.; Volokh, K. Mechanics of Physically Cross-Linked Hydrogels: Experiments and Theoretical Modeling. *Macromolecules* **2025**, *58* (9), 4478–4487. <https://doi.org/10.1021/acs.macromol.5c00486>.
- (46) Winter, H. H. Evolution of Rheology during Chemical Gelation. In *Permanent and Transient Networks*; Springer, 2007; pp 104–110.
- (47) Hess, W.; Vilgis, T. A.; Winter, H. H. Dynamical Critical Behavior during Chemical Gelation and Vulcanization. *Macromolecules* **1988**, *21* (8), 2536–2542.

- (48) Winter, H. H. Evolution of Rheology during Chemical Gelation. In *Permanent and Transient Networks*; Steinkopff: Darmstadt; pp 104–110.
<https://doi.org/10.1007/BFb0109413>.
- (49) Aime, S.; Cipelletti, L.; Ramos, L. Power Law Viscoelasticity of a Fractal Colloidal Gel. *J Rheol (N Y N Y)* **2018**, 62 (6), 1429–1441.

Supporting Information

Dual Cross-Linked Hydrogels: Linear Rheology and Fractional Calculus Modeling

Agniva Dutta^a, Valeriy V. Ginzburg^{b,*}, Gleb Vasilyev^a, and Eyal Zussman^{a,*}

^a NanoEngineering Group, Faculty of Mechanical Engineering, Technion-Israel Institute of Technology, Haifa 3200003, Israel

^b Department of Chemical Engineering and Materials Science, Michigan State University, East Lansing, Michigan 48224, USA

* Corresponding author emails: ginzbur7@msu.edu (VVG), meeyal@me.technion.ac.il (EZ)

1. Amplitude sweep and the boundaries of the linear region

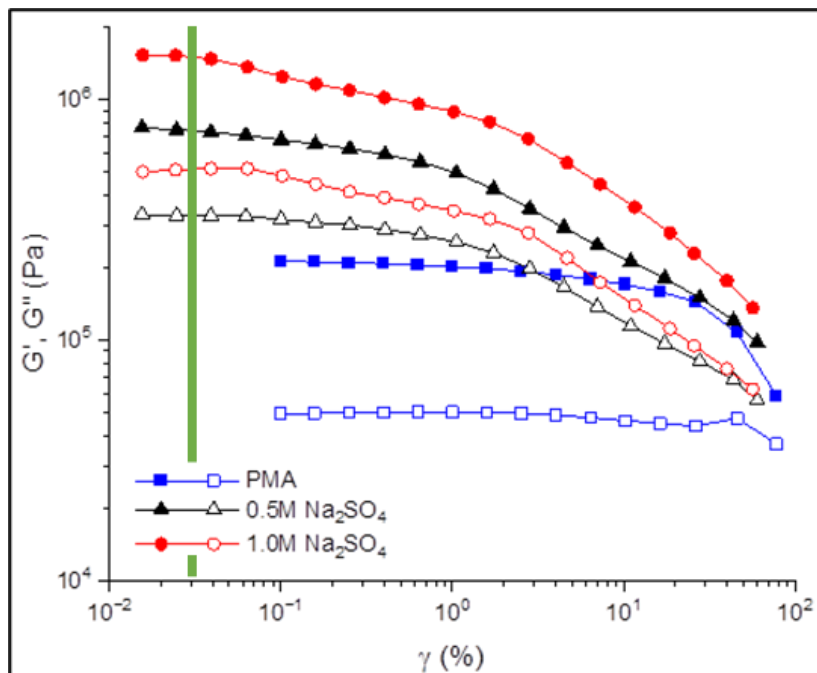


Figure S1. The results of the amplitude sweep tests for the hydrogels show a narrowing of the region of linear viscoelastic response of the materials with the increase of the salt concentration. The green line corresponds to the strain amplitude used in the oscillatory shear tests (0.04%).

Figure S1 shows the amplitude sweep (storage and loss moduli) for three gels: PMA (no salt), 0.5M Na_2SO_4 PMA, and 1M Na_2SO_4 PMA. Based on these curves, we can estimate the boundaries of the linear region (where the G' begins to deviate significantly from the initial plateau) as: PMA (no salt) – 5-10%; 0.5M Na_2SO_4 – 0.1-0.3%; and 1M Na_2SO_4 – 0.05-0.1%.